

Journal of Biological Control, 39(2): 219-226, 2025, DOI: 10.18311/jbc/2025/47955

Research Article

Green synthesis of silver nanoparticles using *Solanum pubescens* leaf and its *in vitro* antifungal activity against *Sclerotium rolfsii*

MANSOUR ABDEL RAHMAN AHMAD ALJABALI*, V. BASAVARAJ, M. R. SAMPATHKUMAR and M. S. SHARADA

Department of Studies in Botany, Manasagangotri, University of Mysore, Mysuru – 570006, Karnataka, India
**Corresponding author E-mail:* mansouraljabali4@gmail.com

ABSTRACT: Soil-borne pathogens, such as *Sclerotium rolfsii*, pose significant threat to agricultural productivity, causing southern blight and leading to severe economic losses. This study explores the green synthesis of silver nanoparticles (Ag-NPs) using *Solanum pubescens* leaf extract as an eco-friendly and sustainable alternative to chemical fungicides. The synthesis was confirmed through visible colour changes and further characterised using UV-Visible spectroscopy, X-Ray Diffraction (XRD), Fourier Transform Infrared Spectroscopy (FTIR), and Scanning Electron Microscopy (SEM). A distinct surface plasmon resonance peak at 426 nm indicated successful Ag-NP formation, while XRD analysis confirmed their crystalline nature with particle sizes ranging from 38.35 Å to 72.57 Å. FTIR analysis revealed the presence of phenolics, amines, and carbonyl groups, highlighting their role in reducing and stabilising Ag-NPs. SEM images confirmed the spherical morphology of Ag-NPs with average diameters ranging between 73.9 and 99.2 nm. The antifungal activity of synthesized Ag-NPs was evaluated *in vitro* using the poisoned food technique against *S. rolfsii*. Ag-NPs at concentrations of 25, 50, and 100 mg/L exhibited significant inhibition of mycelial growth compared to untreated controls and the standard fungicide Mancozeb. The highest inhibition was observed at 100 mg/L, demonstrating the efficacy of green-synthesised Ag-NPs in controlling fungal pathogens. These findings highlight the potential of *S. pubescens*-mediated Ag-NPs as an effective, eco-friendly alternative for managing soil-borne diseases like southern blight, paving way for environmentally safe disease management strategies in agriculture.

Keywords: Antifungal activity, *Sclerotium rolfsii*, soil-borne, *Solanum pubescens*, silver-nanoparticles

(Article chronicle: Received: 28-12-2024; Revised: 15-04-2025; Accepted: 17-04-2025)

INTRODUCTION

Soil-borne fungal pathogens pose a major challenge to agricultural productivity, with diseases such as southern blight caused by *Sclerotium rolfsii* leading to severe economic losses across various crops. Traditional management strategies, including chemical fungicides, are effective but face several challenges. These include the emergence of fungicide-resistant strains, potential toxicity to non-target organisms, and risks associated with fungicide residues that threaten environmental and human health (Sharon *et al*., 2010). In response, there is an urgent need for sustainable, eco-friendly alternatives to conventional fungicides.

Nanotechnology offers a promising solution, with Nanoparticles (NPs) demonstrating superior efficacy compared to synthetic chemicals due to their unique physicochemical properties. Among them, silver nanoparticles (Ag-NPs) are particularly significant for their broad-spectrum antimicrobial activity, which stems from their high surface area-to-volume ratio, enhanced interaction with microbial cells, and distinctive mechanisms of pathogen inhibition (Jo *et al*., 2009; Park *et al*., 2006). These mechanisms include disruption of cell membranes, DNA damage, Reactive Oxygen Species (ROS) generation, and enzyme inhibition (Kim *et al*., 2012; Min *et al*., 2009). Ag-NPs are increasingly recognised as environmentally acceptable alternatives for managing plant diseases while minimising ecological impact. Silver nanoparticles exhibit unique properties due to their nanoscale size, morphology, and structure, which enhance their antimicrobial activity compared to their bulk counterparts (Nel *et al*., 2006; Abdel-Monem *et al*., 2020; Mourad *et al*., 2020). The increased surface area and the generation of reactive Ag^+ ions significantly enhance their biological interactions. The antimicrobial properties of Ag-NPs are influenced by their concentration, size, and morphology, as highlighted by Kim *et al*. (2007). Moreover, the nanoscale dimension facilitates

the efficient adhesion of particles to microbial surfaces, saturating pathogen fragments and arresting growth (Samuel & Guggenbichler, 2004).

Conventional methods for synthesising Ag-NPs often involve energy-intensive processes or the use of hazardous chemicals. However, green synthesis, leveraging plant-based reducing and stabilising agents, has emerged as an eco-friendly and scalable alternative. Plant extracts are rich in bioactive compounds such as phenolics, flavonoids, and alkaloids, which facilitate the nucleation and stabilisation of Ag-NPs (Ahmad *et al*., 2002; Narayanan & Sakthivel, 2010; Rehman *et al*., 2020). This method reduces environmental risks and enhances the synthesised nanoparticles' biological activity (Darwesh *et al*., 2020; Elshahawy *et al*., 2018).

This study investigates the green synthesis of Ag-NPs using *Solanum pubescens* leaf extract, a plant known for its bioactive properties (Rahman *et al*., 2014; Rahman *et al*., 2014; Nagaraju & Rao, 1990) and evaluates their antifungal potential against *S. rolfsii* under *in vitro* conditions. Elaborating on previous research that demonstrated the efficacy of Ag-NPs against fungal pathogens such as *Fusarium culmorum*, *Colletotrichum gloeosporioides*, and *Pythium ultimum* (Aguilar-Méndez *et al*., 2011; Marek *et al*., 2010; Park *et al*., 2006), this work aims to contribute to the development of sustainable disease management strategies. The findings hold promise for addressing the challenges of fungal diseases while supporting environmentally safe agricultural practices.

MATERIALS AND METHODS

Green synthesis of silver nanoparticles (Ag-NPs) using *S. pubescens* leaf extract collection and preparation of leaf extract

Leaves of *S. pubescens* were collected from healthy plants from the Gopinatham forest region (12.0524° N, 77.6987° E), Chamarajanagara district, Karnataka state, India. The collected leaves were washed thoroughly with distilled water to remove dirt and debris, cut into small pieces, and air dried at room temperature. then the dried leaves were powdered using a blender. Ten grams of this powder was boiled in 100 mL of distilled water for 20 min on a hot plate. The mixture was cooled and filtered using Whatman No. 42 filter paper, and the filtrate was stored for nanoparticle synthesis (Khatoon *et al*., 2024).

Synthesis of silver nanoparticles

For Ag-NP synthesis, 20 mL of the prepared *S. pubescens* leaf extract was mixed with 80 mL of 1 mM silver nitrate ($AgNO_3$) solution. The mixture was incubated at room temperature, and the colour change from light brown to dark brown was monitored, indicating the formation of Ag-NPs. After 24 h, the solution was centrifuged at 9000 rpm for 15 min. The supernatant was discarded, and the nanoparticle pellet was freeze-dried to obtain powdered Ag-NPs, which were used for characterisation and antifungal activity testing (Khatoon *et al*., 2024).

Characterisation of Ag-NPs

UV-visible spectroscopy

UV-Vis spectrophotometric analysis confirmed Ag-NP synthesis by measuring absorbance in the 300–800 nm range. The characteristic surface plasmon resonance peak was recorded after 24 hours using the DU® 730 Life Science UV/Vis Spectrophotometer available at the Institution of Excellence (IOE), Vijnana Bhavana, Manasagangotri, Mysuru (Singh *et al*., 2010).

X-Ray Diffraction (XRD)

The crystalline structure of freeze-dried Ag-NPs was analysed using XRD (Bruker, Germany) available at the Institution of Excellence (IOE), Vijnana Bhavana, Manasagangotri, Mysuru (Singh *et al*., 2010).

Fourier Transform Infrared Spectroscopy (FTIR)

Fourier Transform Infrared Spectroscopy (FTIR) analysis was performed to identify functional groups responsible for reducing and capping Ag-NPs. Freeze-dried Ag-NPs were mixed with potassium bromide (KBr) and analysed using a Spectrum Two ($LiTaO_3$ Detector) spectrometer over a 400–4000 cm^{-1} range available at the Institution of Excellence (IOE), Vijnana Bhavana, Manasagangotri, Mysuru (Singh *et al*., 2010).

Scanning Electron Microscopy (SEM)

The morphology of Ag-NPs was analysed using SEM. A small amount of Ag-NP powder was placed on a carbon-coated copper grid, dried under a mercury lamp, and examined using an EVO MA 15 (Carl Zeiss, Germany) electron scanning microscope available at the Institution of Excellence (IOE), Vijnana Bhavana, Manasagangotri, Mysuru (Singh *et al*., 2010).

Antifungal activity of green-fabricated AgNPs

Isolation and identification of *S. rolfsii*

S. rolfsii, the causal agent of root rot in various crops, was isolated from infected tomato plants collected during a survey in the Mysuru region of Karnataka, India. Diseased samples were washed to remove debris, surface sterilised, and plated on PDA medium. Plates were incubated at 27 ± 2°C for 5-7 days, and pure colonies of *S. rolfsii* were obtained through subculturing. Identification was based on morphological features such as mycelial growth pattern, sclerotial size, colour, and shape (Mahadevakumar & Janardhana, 2016).

In vitro Petri plate assay

The antifungal activity of green-synthesised Ag-NPs was evaluated against *S. rolfsii* using the poisoned food technique. PDA medium was amended with different concentrations of Ag-NPs (25, 50, and 100 mg/L), $AgNO_3$ (1 mM), and a standard fungicide (mancozeb, 2 g/L). Untreated plates served as controls. A 7-mm agar plug of *S. rolfsii* was placed in the centre of each plate, and the plates were incubated at 27 ± 2°C for a week. The radial mycelial growth of the pathogen was measured (Khatoon *et al*., 2024; Kaman & Dutta, 2019).

Calculation and statistical analysis

The percentage inhibition of *S. rolfsii* growth was calculated using the formula:

$$Inhibition\ (\%) = \frac{C - T}{C} \times 100$$

where, C is the radial growth in control plates and T is the radial growth in treated plates. Experiments were conducted in five replicates to ensure reliability. Data were analysed statistically analysed (one-way ANOVA) using OPSTAT, which is available online at CCSHAU, Hisar website (www.hau.ac.in).

RESULTS

Green synthesis of silver nanoparticles using *S. pubescens* leaf extract

The synthesis of silver nanoparticles (Ag-NPs) using a green approach was initially confirmed through a visible colour change in the colloidal solution containing leaf extract and $AgNO_3$. The $AgNO_3$ solution appeared nearly transparent, while the leaf extract filtrate exhibited a light brown colour. Upon mixing the two, the solution turned brown. After 24 h of reaction, the mixture developed a dark brown colour, indicating the successful formation of Ag-NPs (Figure 1). This characteristic colour change to dark brown is attributed to the unique optical properties of Ag-NPs, which are influenced by electron oscillation and the Surface Plasmon Resonance (SPR) phenomenon associated with the nanoparticles.

Characterisation of green-synthesised Ag-NPs

UV-Spectrophotometer

The successful synthesis of silver nanoparticles (Ag-NPs) using *S. pubescens* leaf extract was confirmed through UV-Vis spectroscopy. A distinct surface plasmon resonance (SPR) peak was observed at 426 nm (Figure 2), a characteristic feature of silver nanoparticles, indicating their formation. The intensity of the peak reflects the reduction of silver ions into nanoparticles by phytochemicals present in the leaf extract. The broad nature of the SPR peak suggests a slight variation in nanoparticle size, which is commonly associated with the biomolecule-mediated synthesis process. This analysis highlights the efficient and eco-friendly synthesis of AgNPs using the bioactive components of *S. pubescens*.

X-Ray Diffraction (XRD)

The XRD analysis of green synthesised silver nanoparticles (Ag-NPs) using *S. pubescens* leaf extract revealed key diffraction peaks at 2θ values of 32.46°, 37.60°, 46.24°, and 64.57° were attributed to the (111), (200), (220), and (311) lattice planes respectively (Figure 3). These peaks are indicative of interplanar d-spacings of 2.76 Å, 2.39 Å, 1.96 Å, and 1.44 Å, respectively. The Full Width at Half Maximum (FWHM) values for these peaks ranged from 1.35° to 2.25°, highlighting the crystalline structure of the nanoparticles. The calculated crystallite sizes, using the Scherrer equation, ranged from 38.35 Å to 72.57 Å, confirming the nanometer-scale size of the particles. Among

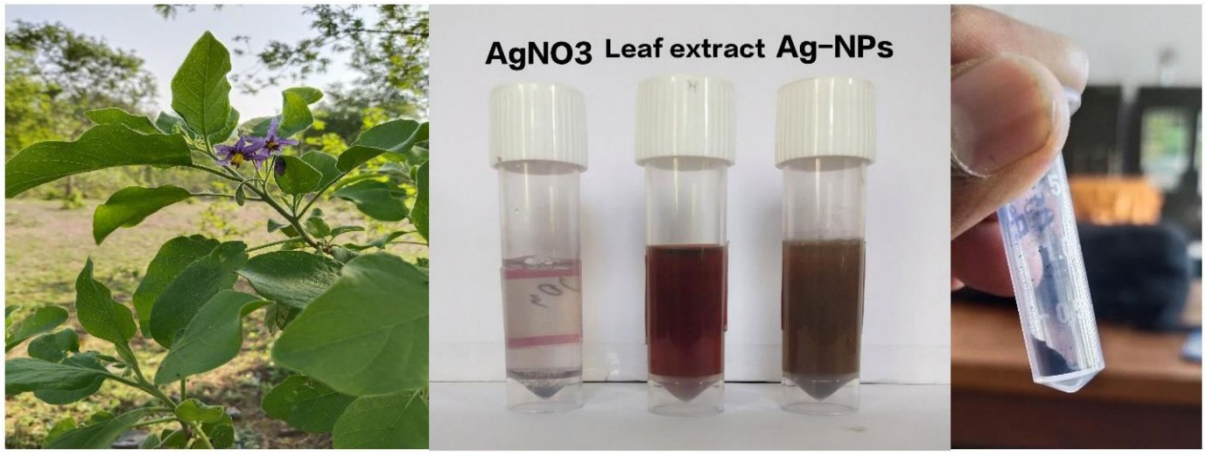


Figure 1. Green synthesis of Ag-NPs using *S. pubescens* leaf extract (*S. pubescens* plant, visual colour change of synthesised Ag-NPs and Synthesised Ag-NPs)**.**

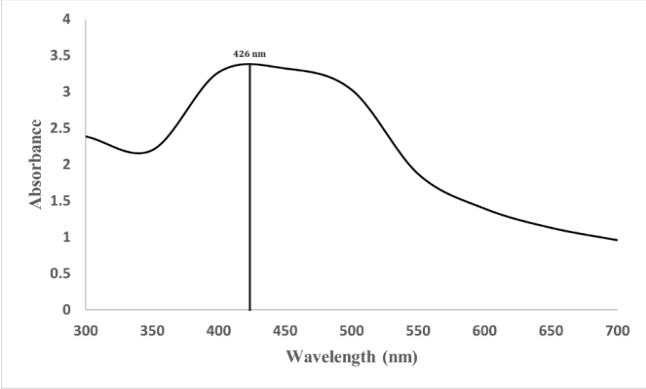


Figure 2. Characterisation of green synthesised Ag-NPs using UV-Vis spectroscopy.

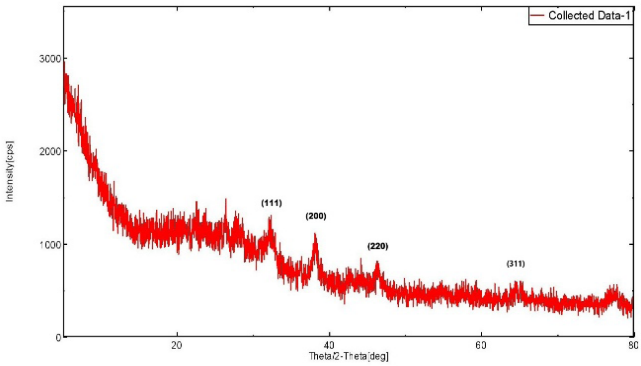


Figure 3. Characterisation of green synthesised Ag-NPs using XRD.

the peaks, the highest intensity was observed at 37.60° with a relative intensity of 100%, indicating a strong reflection. The asymmetric factor and shape of the peaks (split pseudo-Voigt) suggest the presence of slight lattice strain or size variation within the nanoparticles. These results confirm the crystalline nature and nano-dimensional nature of the Ag-NPs synthesised through green synthesis, underscoring the efficacy of *S. pubescens* leaf extract in reducing and stabilising silver ions.

Fourier Transform Infrared Spectroscopy (FTIR)

The Fourier Transform Infrared (FTIR) analysis of silver nanoparticles (Ag-NPs) synthesised using *S. pubescens* leaf extract identified various functional groups responsible for the reduction and stabilisation of the nanoparticles. A broad peak at 3714.68 cm^{-1} with a transmittance of 96.44% corresponds to the stretching vibrations of hydroxyl (-OH) groups, suggesting the presence of phenolics and alcohols. The peak at 3216.45 cm^{-1} (94.25% transmittance) is attributed to N-H stretching vibrations of amines or amide groups, suggesting the involvement of proteins. The peak at 2180.92 cm^{-1} (95.93% transmittance) represents C≡C stretching of alkynes, while the peak at 1979.32 cm^{-1} (95.93% transmittance) is associated with C=O stretching of carbonyl groups. A strong peak at 1578.44 cm^{-1} (93.01% transmittance) indicates the presence of aromatic C=C stretching, likely due to flavonoids or other aromatic compounds. Peaks at 1305.32 cm^{-1} (91.26% transmittance) correspond to C-N stretching vibrations of amines, suggesting protein interactions in the synthesis process. Additionally, significant peaks at 631.86 cm^{-1} (91.96%), 620.98 cm^{-1} (91.09%), and 603.97 cm^{-1} (91.71%) can be assigned to C-H bending or alkyl halides (Figure 4). These functional groups underscore the variety of biomolecules in the leaf extract that serve as reducing and capping agents in the biosynthesis of Ag-NPs. This confirms the eco-friendly and phytochemical-mediated synthesis of Ag-NPs.

Scanning Electron Microscope (SEM)

Scanning Electron Microscopy (SEM) was employed to examine the surface morphology of the green-synthesised Ag-NPs. The SEM analysis of the Ag-NPs synthesised using *S. pubescens* leaf extract revealed the presence of spherical nanoparticles. The average diameter of the synthesised Ag-NPs ranged from 73.9 to 99.2 nm (Figure 5).

In vitro antifungal activity of Ag-NPs against S. rolfsii

The antifungal efficacy of green synthesised silver nanoparticles (Ag-NPs) using *S. pubescens* leaf extract against *S. rolfsii* was evaluated through a Petri plate assay at various concentrations (25 ppm, 50 ppm, and 100 ppm). The untreated control exhibited a colony diameter of 89.20 ± 0.374 mm, while treatments with Ag-NPs effectively inhibited fungal growth. At 25 ppm, the colony diameter.

was reduced to 20.40 ± 1.030 mm, corresponding to 77.13% control. Increasing the concentration to 50 ppm further decreased the colony diameter to 10.40 ± 1.122 mm (88.34% control), and at 100 ppm, the highest inhibition was observed, with a colony diameter of 7.80 ± 1.068 mm and 91.25% control. In comparison, $AgNO_3$ showed negligible antifungal activity, with a colony diameter of 88.60 ± 0.245 mm and only 0.67% control. The fungicide (Mancozeb) used as a standard exhibited the highest efficacy, with a

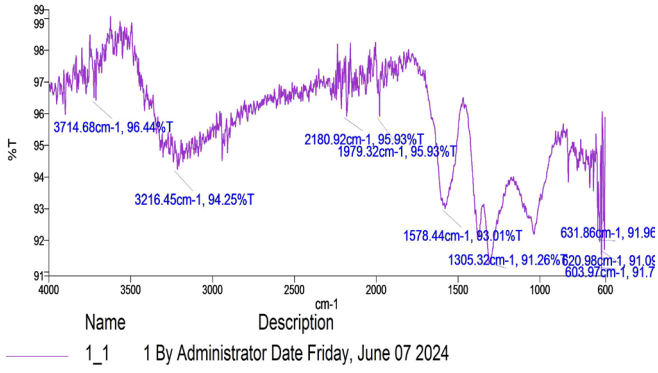


Figure 4. Characterisation of green synthesised Ag-NPs using FTIR.

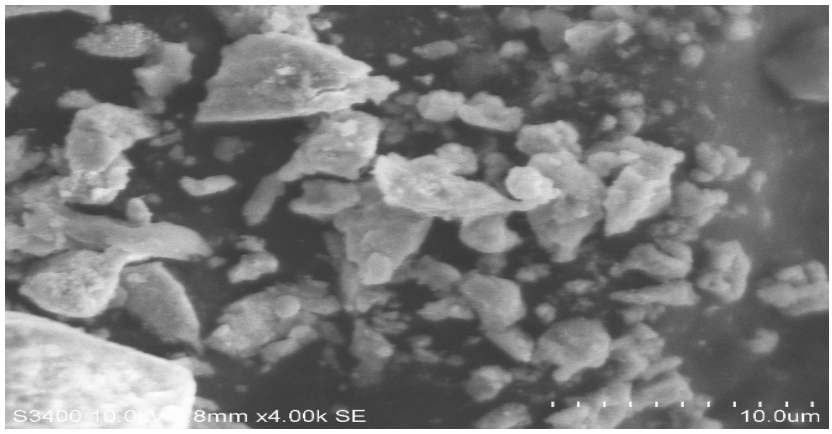


Figure 5. Characterisation of green synthesised Ag-NPs - Scanning Electron Microscopic (SEM) images of green synthesised Ag-NPs.

Table 1. Antifungal activity (Petri plate assay) of green synthesised Ag-NPs using *S. pubescens* leaf extract against *S. rolfsii* (Values are mean of five replications with standard error (±) and per cent control over untreated control)

Concentration	Control (0%)	Silver nanoparticles			$AgNO_3$	Fungicide
		25 ppm	50 ppm	100 ppm		
Colony Diameter (mm)	89.20 ± 0.374	20.40 ± 1.030	10.40 ± 1.122	7.80 ± 1.068	88.60 ± 0.245	6.20 ± 0.663
Percent Control	-	77.13 %	88.34 %	91.25 %	0.67 %	93.04 %

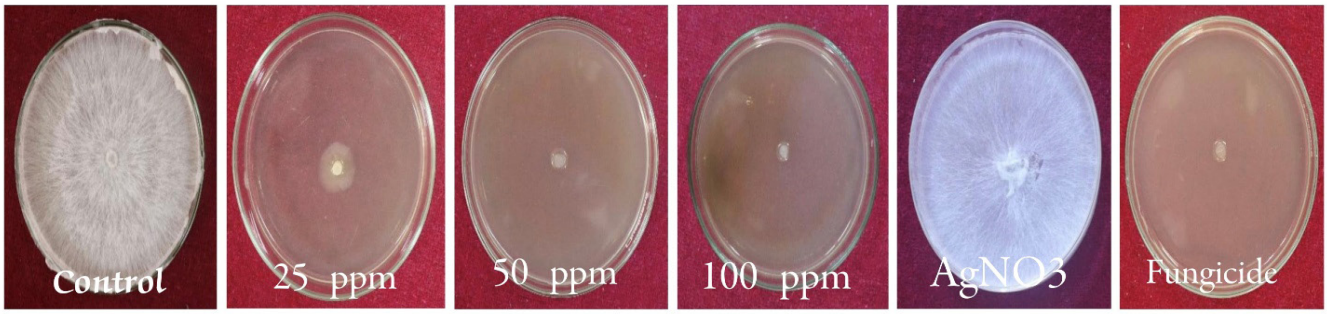


Figure 6. Antifungal activity of green synthesised Ag-NPs against *S. rolfsii* under *in vitro* Petri plate assay.

colony diameter of 6.20 ± 0.663 mm and 93.04% control (Table 1, Figure 6). These results highlight the potential of *S. pubescens*-mediated Ag-NPs as a potent antifungal agent against *S. rolfsii*, with effectiveness comparable to chemical fungicides at higher concentrations.

DISCUSSION

The green synthesis of silver nanoparticles (Ag-NPs) using *S. pubescens* leaf extract represents a sustainable and eco-friendly approach. The formation of Ag-NPs is indicated by a distinct dark brown colour, a hallmark of Surface Plasmon Resonance (SPR), confirming the reduction of silver ions by phytochemicals in the extract. This finding aligns with previous reports highlighting the role of bioactive compounds in the reduction and stabilisation of nanoparticles (Khatoon *et al*., 2024; Khalil *et al*., 2023).

UV-Vis spectroscopy revealed an SPR peak at 426 nm, consistent with the characteristic range of silver nanoparticles. Similar peaks have been reported for Ag-NPs synthesised using *S. trilobatum* (430 nm; Manimegalai *et al*., 2022) and *S. nigrum* (405.97 nm; Jenifer *et al*., 2020). The variation in peak width suggests heterogeneity in particle size, a well-documented feature of biologically synthesised nanoparticles (Zubair *et al*., 2022; Kanniah *et al*., 2020; Perveen *et al*., 2021; Zubair *et al*., 2022). FTIR spectroscopy identified functional groups such as hydroxyl, amine, carbonyl, and aromatic compounds, primarily derived from phenolics, proteins, and flavonoids. These biomolecules act as reducing and capping agents, a mechanism well-supported in the literature (Mourdikoudis *et al*., 2018; Venu *et al*., 2011). XRD analysis confirmed the crystalline nature of the Ag-NPs, with diffraction peaks indicative of nanometer-scale crystallites. Structural integrity, validated through crystallite size and lattice strain calculations, is critical for the biological efficacy of Ag-NPs, as corroborated by previous studies (Goyal *et al*., 2018; Marimuthu *et al*., 2011). SEM revealed that the synthesised Ag-NPs predominantly exhibit

a spherical morphology, with nanoscale dimensions suitable for microbial interactions (Rashid *et al*., 2019; Dwivedi *et al*., 2014). Similar morphological features were observed in Ag-NPs synthesised using *Caesalpinia coriaria* leaf extract, with particle sizes ranging from 40.90 to 52.76 nm (Jeeva *et al*., 2014).

The antifungal efficacy of green-synthesised Ag-NPs was demonstrated against *S. rolfsii*, with growth inhibition reaching 91.25% at 100 ppm. This concentration-dependent antifungal activity is consistent with findings from Min *et al*. (2009) and Jung *et al*. (2010), where biologically synthesised Ag-NPs inhibited the growth of *Stromatinia cepivora*. The antifungal mechanism involves Ag-NP interactions with fungal cell membranes, leading to structural disruption and functional impairment (Kim *et al*., 2007). Silver ions (Ag^+) inactivate membrane-bound enzymes, such as those in the respiratory chain, further disrupting fungal metabolism (Kim *et al*., 1998; McDonnell & Russell, 1999). The enhanced reactivity of Ag-NPs is attributed to their nanoscale properties, enabling efficient cell penetration and Ag^+ ion release. These ions interact with oxygen to generate ROS, which damages microbial proteins, lipids, and nucleic acids (Storz & Imlay, 1999; Hwang *et al*., 2008). Lamsal *et al*. (2011) reported structural alterations in fungal hyphae, including cell wall deformation and membrane damage, following Ag-NP exposure. Notably, the efficacy of Ag-NPs remains significant even at lower concentrations. For example, Ag-NPs synthesised from *Trichoderma asperellum* achieved 78.36% fungal inhibition at 100 ppm (Kaman & Dutta, 2019).

The potential of Ag-NPs as a safer and more effective alternative to conventional fungicides has gained considerable attention. Green-synthesised nanoparticles exhibit broad-spectrum biocidal activity against plant pathogens, with some outperforming commercial fungicides in growth inhibition assays (Mohamed *et al*., 2015; Abdelhameed *et al*., 2019; Panpatte & Jhala, 2019). For instance, Vrandečić *et al*. (2019) reported superior antifungal effects of Ag-NPs compared to certain synthetic fungicides. Additionally, the use of biosynthesised Ag-NPs presents minimal environmental and health risks, making them a promising alternative for sustainable plant disease management.

CONCLUSION

This study establishes *S. pubescens* leaf extract as a viable medium for the green synthesis of Ag-NPs, providing an environmentally friendly alternative for disease management with strong antifungal activity. By harnessing the bioactive compounds in *S. pubescens*, this method aligns with sustainable practices in agricultural pathogen management. Future research should explore field-scale applications, long-term stability, and broader-spectrum efficacy to validate the practical utility of these green-synthesised Ag-NPs in mitigating plant diseases caused by pathogenic fungi.

REFERENCES

Abdelhameed, R. M., Darwesh, O. M., Rocha, J., and Silva, A. M. 2019. IRMOF-3 biological activity enhancement by post-synthetic modification. *Eur J Inorg Chem*, **2019**(9): 1243-1249. https://doi.org/10.1002/ejic.201801442

Abdel-Monem, R. A., Khalil, A. M., Darwesh, O. M., Hashim, A. I., and Rabie, S. T. 2020. Antibacterial properties of carboxymethyl chitosan Schiff-base nanocomposites loaded with silver nanoparticles. *J Macromol Sci A*, **57**(2): 145-155. https://doi.org/10.1080/10601325.2019.1674666

Aguilar-Méndez, M. A., Martín-Martinez, E. S., Ortega-Arroyo, L., Cobián-Portillo, G., and Sánchez-Espíndola, E. 2011. Synthesis and characterization of silver nanoparticles: Effect on phytopathogen *Colletotrichum gloesporioides*. *J Nanoparticle Res*, **13**: 2525-2532.

Ahmad, P., Mukherjee, S., Senapati, D., Mandal, M. I., Khan, R., and Kumar, M. 2002. Extracellular biosynthesis of silver nanoparticles using the fungus *Fusarium oxysporum*. *Colloids Surf B*, **28**, 313-318. https://doi.org/10.1016/S0927-7765(02)00174-1

Darwesh, O. M., Ali, S. S., Matter, I. A., Elsamahy, T., and Mahmoud, Y. A. 2020. Enzymes immobilization onto magnetic nanoparticles to improve industrial and environmental applications. *Methods Enzymol*, **630**: 481-502. https://doi.org/10.1016/bs.mie.2019.11.006

Dwivedi, P., Narvi, S. S., and Tewari, R. P. 2014. Phytofabrication characterization and comparative analysis of Ag nanoparticles by diverse biochemicals from *Elaeocarpus ganitrus* Roxb., *Terminalia arjuna* Roxb., *Pseudotsuga menzietii*, *Prosopis spicigera*, *Ficus religiosa*, *Ocimum sanctum*, *Curcuma longa*. *Ind Crop Prod*, **54**: 22-31. https://doi.org/10.1016/j.indcrop.2013.12.050

Elshahawy, I., Abouelnasr, H. M., Lashin, S. M., and Darwesh, O. M. 2018. First report of *Pythium aphanidermatum* infecting tomato in Egypt and its control using biogenic silver nanoparticles. *J Plant Prot Res*, **15**(2): 137-151. https://doi.org/10.24425/122929

Goyal, M., Kumar, S., Bahadur, I., Verma, C., and Ebenso, E. E. 2018. Organic corrosion inhibitors for industrial cleaning of ferrous and non-ferrous metals in acidic solutions: A review. *J Mol Liq*. **256**:565-573.

Hwang, E. T., Lee, J. H., Chae, Y. J., Kim, Y. S., Kim, B. C., Sang, B. I., and Gu, M. B. 2008. Analysis of the toxic mode of action of silver nanoparticles using stress-specific bioluminescent bacteria. *Small*, **4**: 746-750.

Jeeva, K., Thiyagarajan, M., Elangovan, V., Geetha, N., Venkatachalam, P. 2014. *Caesalpinia coriaria* leaf extracts mediated biosynthesis of metallic silver nanoparticles and their antibacterial activity against clinically isolated pathogens. *Ind Crop Prod*, **52**: 714-720. https://doi.org/10.1016/j.indcrop.2013.11.037

Jenifer, A. A., Malaikozhundan, B., Vijayakumar, S., Anjugam, M., Iswarya, A., and Vaseeharan, B. 2020. Green synthesis and characterization of silver nanoparticles (AgNPs) using leaf extract of *Solanum nigrum* and assessment of toxicity in vertebrate and invertebrate aquatic animals. *J Clust Sci*, **31**: 989-1002. https://doi.org/10.1007/s10876-019-01704-7

Jo, Y. K., Kim, B. H., and Jung, G. 2009. Antifungal activity of silver ions and nanoparticles on phytopathogenic fungi. *Plant Dis*, **93**: 1037-1043. https://doi.org/10.1094/PDIS-93-10-1037

Jung, J. H., Kim, S. W., Min, J. S., Kim, Y. J., Lamsal, K., Kim, K. S., and Lee, Y. S. 2010. The effect of nano-silver liquid against the white rot of green onion caused by *Sclerotium cepivorum*. *Mycobiol*, **38**: 39-45.

Kaman, P. K., and Dutta, P. 2019. Synthesis, characterization and antifungal activity of biosynthesized silver nanoparticle. *Indian Phytopathol,* **72**: 79-88. https://doi.org/10.1007/s42360-018-0081-4

Kanniah, P., Radhamani, J., Chelliah, P., Muthusamy, N., Emmanual, J. J. S. B. T., Reeta, T., and Shanmugam, R. 2020. Green synthesis of multifaceted silver nanoparticles using the flower extract of *Aerva lanata* and evaluation of its biological and environmental applications. *Chem Select*, **5**(7): 2322-2331.

Khalil, S., Mehmood, A., Khan, M. A. R., Ahmad, K. S., Abasi, F., Raffi, M., …, Abdelkarim, M. 2023. Antibacterial, antioxidant and photocatalytic activity of novel *Rubus ellipticus* leaf mediated silver nanoparticles. *J Saudi Chem Soc*, **27**(1): Article 101576.

Khatoon, J., Mehmood, A., Khalid, A. U. R., Khan, M. A. R., Ahmad, K. S., Amjad, M. S., and Proćków, J. 2024. Green-fabricated silver nanoparticles from *Quercus incana* leaf extract to control the early blight of tomatoes caused by *Alternaria solani*. *BMC Plant Biol*, **24**(1): Article 302. https://doi.org/10.1186/s12870-024-05008-5

Kim, J. S., Kuk, E., Yu, K. N., Kim, J. H., Park, S. J., Lee, H. J., …, Cho, M. H. 2007. Antimicrobial effects of silver nanoparticles. *Nanomed: Nanotechnol Biol Med*, **3**(1): 95-101. https://doi.org/10.1016/j.nano.2006.12.001

Kim, S. W., Jung, J. H., Lamsal, K., Kim, Y. S., Min, J. S., and Lee, Y. S. 2012. Antifungal effects of silver nanoparticles (AgNPs) against various plant pathogenic fungi. *Mycobiol*, **40**: 53-58.

Kim, T., Feng, Q., Kim, J., Wu, J., Wang, H., Chen, G. C., and Cui, F. Z. 1998. Antimicrobial effects of metal ions (Ag+, Cu2+, Zn2+) in hydroxyapatite. *J Mater Sci: Mater Med*, **9**: 129-134.

Lamsal, K., Kim, S. W., Jung, J. H., Kim, Y. S., Kim, Y. S., and Lee, Y. S. 2011. Application of silver nanoparticles for the control of *Colletotrichum* species *in vitro* and pepper anthracnose disease in field. *Mycobiol*, **39**: 194-199. https://doi.org/10.5941/MYCO.2011.39.3.194

Mahadevakumar, S., and Janardhana, G. R. 2016. Morphological and molecular characterization of *Sclerotium rolfsii* associated with leaf blight disease of *Psychotria nervosa* (Wild Coffee). *J Plant Pathol*, **98**(2): 351-354. http://www.jstor.org/stable/44280457

Manimegalai, S., Rajeswari, V. D., Parameswari, R., Nicoletti, M., Alarifi, S., & Govindarajan, M. (2022). Green synthesis, characterization and biological activity of Solanum trilobatum-mediated silver nanoparticles. *Saudi Journal of Biological Sciences*, *29*(4), 2131-2137.https://doi.org/10.1016/j.sjbs.2021.11.048

Marek, J. K., Magdalena, K., and Gorczyca, A. 2010. The effect of silver nanoparticles on phytopathogenic spores of *Fusarium culmorum*. *Can J Microbiol*, **56**(3): 247-253. https://doi.org/10.1139/w10-012

Marimuthu, S., Rahuman, A. A., Rajakumar, G., Santhoshkumar, T., Kirthi, A. V., Jayaseelan, C., and Kamaraj, C. 2011. Evaluation of green synthesized silver nanoparticles against parasites. *Parasitol Res*, **108**: 1541-1549.

McDonnell, G., and Russell, A. D. 1999. Antiseptics and disinfectants: Activity, action, and resistance. *Clin Microbiol Rev*, **12**: 147-179.

Min, J. S., Kim, K. S., Kim, S.W., Jung, J. H., Lamsal, K., Kim, S. B., …, Lee, Y. S. 2009. Effects of colloidal silver nanoparticles on sclerotium-forming phytopathogenic fungi. *Plant Pathol J*, **25**(4): 376-380. https://doi.org/10.5423/PPJ.2009.25.4.376

Mohamed, A. A., Ali, S. I., Darwesh, O. M., El-Hallouty, S. M., and Sameeh, M. Y. 2015. Chemical compositions, potential cytotoxic and antimicrobial activities of *Nitraria retusa* Methanolic extract sub-fractions. *Int J Toxicol Pharmacol Res*, **7**(4): 204-212.

Mourad, R. M., Darwesh, O. M., and Abdel-Hakim, A. 2020. Enhancing physico-mechanical and antibacterial properties of natural rubber using synthesized Ag-SiO_2 nanoparticles. *Int J Biol Macromol*, **164**: 3243-3249. https://doi.org/10.1016/j.ijbiomac.2020.08.063

Mourdikoudis, S., Pallares, R. M., and Thanh, N. T. K. 2018. Characterization techniques for nanoparticles: Comparison and complementarity upon studying nanoparticle properties. *Nanoscale*, **27**(10): 12871-12934.

Nagaraju, N., and Rao, K. N. 1990. A survey of plant crude drugs of Rayalaseema, Andhra Pradesh, India. *J Ethnopharmacol*, **29**(2): 137-158.

Narayanan, K. B., and Sakthivel, N. 2010. Biological synthesis of metal nanoparticles by microbes. *Adv Colloid Interface Sci*, **156**(1-2): 1-13.

Nel, A., Xia, T., Mädler, L., and Li, N. 2006. Toxic potential of materials at the nano level. *Science*, **311**: 622-627.

Panpatte, D. G., and Jhala, Y. K. 2019. *Nanotechnology for agriculture: Advances for sustainable agriculture* (p. 305). Springer Nature Singapore.

Park, H. J., Kim, S. H., Kim, H. J., and Choi, S. H. 2006. A new composition of nanosized silica-silver for control of various plant diseases. *Plant Pathol J*, **22**: 295-302.

Perveen, R., Shujaat, S., Naz, M., Qureshi, M. Z., Nawaz, S., Shahzad, K., and Ikram, M. 2021. Green synthesis of antimicrobial silver nanoparticles with Brassicaceae seeds. *Mater Res Express*, **8**(5): Article 055007.

Rahman, H., Mahmood, R., Rahman, N., and Haris, M. 2014. Antibacterial activity of *Solanum pubescens* - An ethnomedicinal plant from South Western region of Andhra Pradesh. *Int J Appl Sci Biotechnol*, **2**(4): 501-509.

Rahman, H. U., Mahmood, R., Haris, M., and Rahman, N. 2014. Phytochemical profiling of successive extracts of fruit and stem bark of *Solanum pubescens*. *Int J Pharm Pharm Sci*, **6**(9): 147-153.

Rashid, S., Azeem, M., Khan, S. A., Shah, M. M., and Ahmad, R. 2019. Characterization and synergistic antibacterial potential of green synthesized silver nanoparticles using aqueous root extracts of important medicinal plants of Pakistan. *Colloids Surf B*, **179**: 317-325.

Rehman, S., Farooq, R., Jermy, R., Ravinayagam, V., Al Jindan, R., Alsalem, Z. H., …, Khan, F. A. 2020. A wild *Fomes fomentarius* for biomediation of one pot synthesis of titanium oxide and silver nanoparticles for antibacterial and anticancer application. *Biomolecules*, **10**: Article 622. https://doi.org/10.3390/biom10040622

Samuel, U., and Guggenbichler, J. P. 2004. Prevention of catheter related infections: The potential of a new nano-silver impregnated catheter. *Int J Antimicrob Agents*, **23S1**: S75-S78.

Sharon, M., Choudhary, A. K., and Kumar, R. 2010. Nanotechnology in agricultural diseases and food safety. *J Phytol*, **2**(4): 83-92.

Singh, A., Jain, D., Upadhyaya, M. K., Khandelwal, N., and Verma, H. N. 2010. Green synthesis of silver nanoparticles using *Argemone mexicana* leaf extract and evaluation of their antimicrobial activities. *Digest J Nanomat Biostruct*, **5**(2): 483-489.

Storz, G., and Imlay, J. A. 1999. Oxidative stress. *Curr Opin Microbiol*, **2**: 188-194.

Venu, R., Ramulu, T. S., Anandakumar, S., Rani, V. S., and Kim, C. G. 2011. Bio-directed synthesis of platinum nanoparticles using aqueous honey solutions and their catalytic applications. *Colloids Surf A*, **384**: 733-738.

Vrandečić, K., Ćosić, J., Ilić, J., Ravnjak, B., Selmani, A., Galić, E., …, Vinković, T. 2019. Antifungal activities of silver and selenium nanoparticles stabilized with different surface coating agents. *Pest Manag Sci*, **76**: 2021-2029. https://doi.org/10.1002/ps.5735

Zubair, M., Azeem, M., Mumtaz, R., Younas, M., Adrees, M., Zubair, E., …, Ali S. 2022. Green synthesis and characterization of silver nanoparticles from *Acacia nilotica* and their anticancer, antidiabetic and antioxidant efficacy. *Environ Pollut*, **304**: Article 119249.